Published by IOP Publishing for Sissa Medialab

Received: *October 15, 2019*
Accepted: *December 8, 2019*
Published: *January 23, 2020*

21st International Workshop on Radiation Imaging Detectors
7–12 July 2019
Crete, Greece

SiC based charged particle strip sensor spectrometer with neutron detection capability

T. Slavicek,[a,1] S. Petersson,[a] S. Pospisil,[a] G. Thungstrom[b] and M. Slavickova[a]

[a] *Institute of Experimental and Applied Physics, Czech Technical University in Prague, Husova 240/5, 110 00 Prague, Czech Republic*
[b] *Department of Information Technology and Media, Mid Sweden University, Mittuniversitetet, 852 30 Sundsvall, Sweden*

E-mail: tomas.slavicek@utef.cvut.cz

Abstract: Silicon carbide (SiC) devices have gained much attention owing to their superior characteristics that make them high-temperature and radiation-hard. The advantage of the SiC arises from its unique combination of electronic and physical properties such as a wide band-gap, high breakdown electric field strength, high saturated electron velocity, and high thermal conductivity. The wide band-gap results in a low intrinsic charge carrier concentration and a radiation hardness. The low intrinsic charge carrier concentration leads to low device leakages at high temperature. The high breakdown strength allows SiC devices to operate at much higher voltages. The aim of this publication is to present current status of a charged particle spectrometer based on a SiC strip detector. The sensor is made of a 4H-SiC (α-SiC) hexagonal crystalline structure material which manifests good spectroscopic characteristics for charged particle detection similar to a standard silicon diode (20 keV FWHM with 5,4857 MeV 241Am alpha particle). To obtain sensors for the charged particle detection out of the SiC bulk material we created Schottky contacts on the top and the Ohmic contact on the bottom. Preparation of the contacts will be discussed alongside the electric characterization of the sensor material. Results of the charged particle and the gamma detection and detection of thermal neutron detection (after a neutron converter deposition) will be presented. There will be also a discussion regarding fast neutron detection. The SiC sensor material was attached to a VATA GP8 based 128 strip readout to form the handheld spectrometer which will be demonstrated.

Keywords: Front-end electronics for detector readout; Neutron detectors (cold, thermal, fast neutrons); Particle tracking detectors (Solid-state detectors)

[1] Corresponding author.

© 2020 IOP Publishing Ltd and Sissa Medialab
https://doi.org/10.1088/1748-0221/15/01/C01036

2020 JINST 15 C01036

Contents

1 Introduction **1**

2 Detector design and fabrication **1**
- 2.1 Silicon carbide 1
- 2.2 Front and back side contact 2

3 Characterization of the sensor **3**
- 3.1 Current-Voltage (I-V) measurement 3
- 3.2 Detection tests 3

4 VATA GP8 strip sensor readout **5**
- 4.1 Description of the readout 5
- 4.2 Test results 6

5 Conclusions **7**

1 Introduction

The current state of the nuclear research and the development in an experimental facilities exert pressure on qualities of sensors. Semiconducting sensors are undergoing the permanent development to be able to maintain the pace of increasing requirements on the radiation hardness and the particle tracking capabilities, etc. of experiments at CERN [1] or currently built European Spallation Source.

This article demonstrates a possibility to use a Silicon Carbide (SiC) as a radiation hard sensor of charged particles, non-ionizing particles (neutrons) and presents the application of the sensor in a handheld spectrometer.

The advantage of the SiC arises from its unique combination of an electronic and physical properties. Our sensor is made of 4H-SiC (α-SiC) hexagonal crystalline structure material which manifests good spectroscopic characteristics for charged particle detection similar to a standard silicon. By deposition of a ^{6}LiF neutron converter it acquires a capability of the thermal neutron detection [2] and it is sensitive to a fast neutrons thanks to nuclear reactions of fast neutrons with carbon (^{12}C) and silicon (^{28}Si) atoms.

2 Detector design and fabrication

2.1 Silicon carbide

The wide band-gap of the SiC has an effect of the lower leakage current comparing to the silicon at high temperature. The high breakdown strength allows SiC devices to operate at much higher

2020 JINST 15 C01036

Table 1. Comparison of properties of promising radiation hard materials [1].

Property	**Diamond**	**4H-SiC**	**Si**	**GaN**
E_g (eV)	5.5	3.27	1.12	3.39
$E_{breakdown}$ [V/cm]	10^7	$2.2*10^6$	$3*10^5$	$4*10^6$
μ_e (cm^2 V s^{-1})	1800	800	1500	1000
μ_h (cm^2 V s^{-1})	1200	115	450	30
e-h energy (eV)	13	8.4	3.6	~8–10
Displacement. (eV)	43	25	13–20	~10–20
Density (g cm^{-3})	3.52	3.21	2.33	6.15
Radiation length, X_0 (cm)	12.2	8.7	9.4	2.7
e-h pairs/X_0 (10^6 cm^{-1})	4.4	4.5	10.1	~2–3

voltages. And a higher displacement threshold than the silicon signify that the SiC is radiation harder than the silicon (table 1).

Sensors are made of the 4H-SiC (α-SiC) hexagonal crystalline structure material provided by ACREO (Sweden) (figure 2). A four-inch wafer is of the SiC base material with a micrometre highly doped n+ buffer and 50 micrometres epitaxial layer (n = $5.3*10^{14}$ cm^{-3}). The material for this first production run had quite large amount of defects which resulted in poor break down voltages.

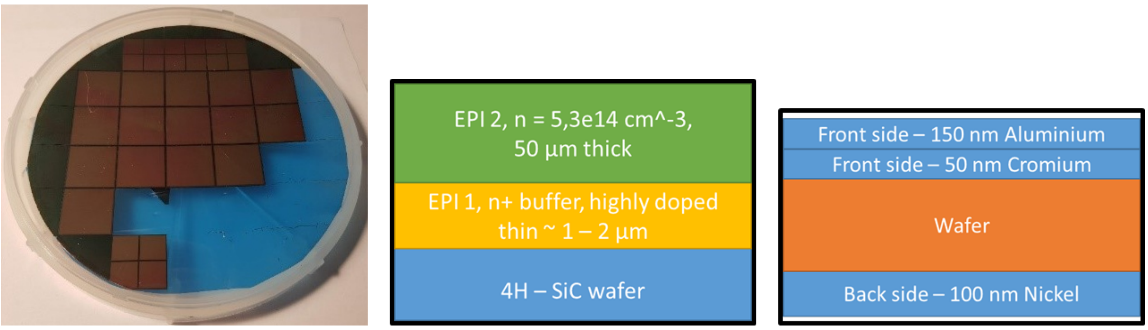

(a) **(b)** **(c)**

Figure 1. (a) The SiC wafer covered by a photoresist after dicing and removal of several sensors. (b) Internal structure of the SiC wafer. (c) Structure of contacts deposited on the SiC wafer.

2.2 Front and back side contact

Fabrication of the sensors such as EB-PVD deposition of contacts, lithography and dicing was done in the clean rooms of Mid Sweden University.

To obtain sensors for the charged particle detection out of the SiC bulk material we created Schottky contacts on the top and the Ohmic contact on the bottom (figure 1). Front Schottky contact was formed by deposition of 50 nm of Chromium. Moreover, we deposited 150 nm of Aluminium for better adhesion during the wire-bonding. We also tested using Titanium layer in

2020 JINST 15 C01036

between Aluminium and Chromium but this resulted in poor selectivity during etching. The back side Ohmic contact was produced by deposition of 100 nm of Nickel.

To test different sensor structures we prepared a photomask for front side of the wafer where half of the wafer were strip sensors and half of the wafer were pixel sensors. Pixel and strip sensors have both 220 µm pitch and are equipped with set of guard rings on the edge of the sensors with the width of 150 µm.

After a first test, an I-V measurement and an alpha spectroscopy, we deposited ^{6}LiF on the front side contact. The deposition was done by an air-brush deposition of mixture of ^{6}LiF, a binder (dispersion glue) and water. This is very reliable technique which allows deposition of fine and thick layers. For thin layers it is better to deposit the ^{6}LiF by sputtering but this method produces a conductive layer whereas the air-brush technique produces non-conductive.

3 Characterization of the sensor

3.1 Current-Voltage (I-V) measurement

Measurement of the I-V curves provided standard results while decreasing and increasing the current. Unfortunately, the material had a lot of defects which resulted in lower breakdown voltage of the strips than expected with SiC.

To measure the I-V characteristic we placed the sensor on a conductive board which acted as back-side contact and used a spring contact which acted as a front-side contact. The spring contact has diameter of about 1 mm, which means that during the measurement of the I-V curves we measured the dependency of several strips (4 strips). The total area of the measured contact was 12,32 μm^2.

Measurement of the I-V curves was done automatically by the Keithley 2410 source meter using a software developed at IEAP CTU in Prague. The source meter was connected to a PC via a GPIB to USB converter. The range of the measured voltage was set from 0 V to -500 V to avoid any problems with sparks or discharges. The voltage was set in 1 V steps and in each step the current was measured three times with measurement period of 1 second. Stored value of the current is average of the three values. There is a current limit so in case there is a sensor breakdown the measurement is interrupted and the voltage is decreased to zero.

Figure 2 shows a comparison between the high grade SiC sensor with the 10 µm epitaxial layer and single pad electrode of 1 mm^2 diameter of front-side electrode (figure 2(a)) provided by SINTEF and our strip sensor. One can clearly see that the quality of the epitaxial layer has a major effect on the shape of the I-V curve and values of the current. Whereas the SINTEF sensor does not exceed 0,7 nA at -500 V and does not show any signs of the breakdown, our sensor reaches about 120 nA at -300 V and show rapid increase of the current which is sign of the breakdown (figure 2(b)).

3.2 Detection tests

Once selected sensors passed the I-V curve measurement, one with the best response was selected to pass an alpha particle detection test. The sensor was attached to a similar holder with the conductive board bottom electrode and the spring contact front electrode and placed in a vacuum chamber. Using the standard spectroscopic chain consisting of a charge sensitive preamplifier (R_s = 110 MΩ,

2020 JINST 15 C01036

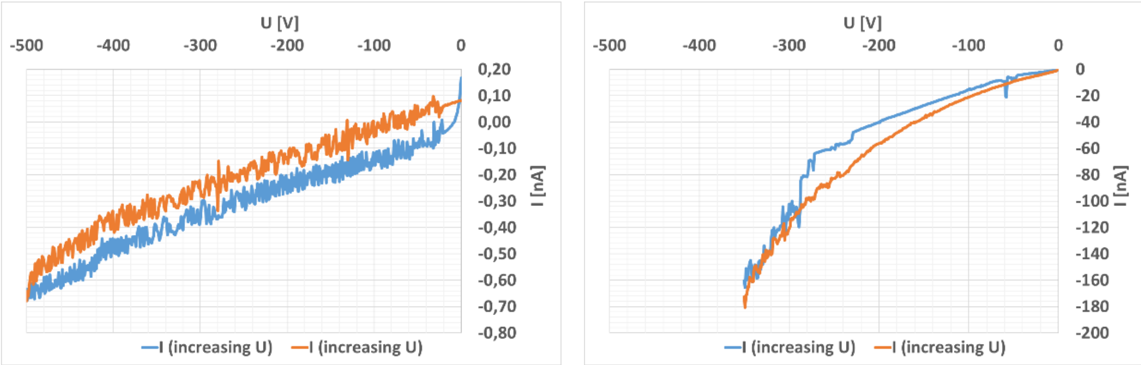

(a) **(b)**

Figure 2. (a) I-V characteristics of the high grade single pad SiC detector (b) I-V characteristics of our SiC strip detector.

C = 1 nF), a spectroscopy amplifier ORTEC 673 (coarse gain 100, shaping 0,25 µs) and Canberra ADC 8715 set to 2K range and gain we measured response to the ^{241}Am alpha source. The response was compared to a standard ORTEC Si PIN diode. We measured the energy resolution of about 20 keV Full-Width-at-Half Maximum (FWHM) comparable between the SiC and the Si.

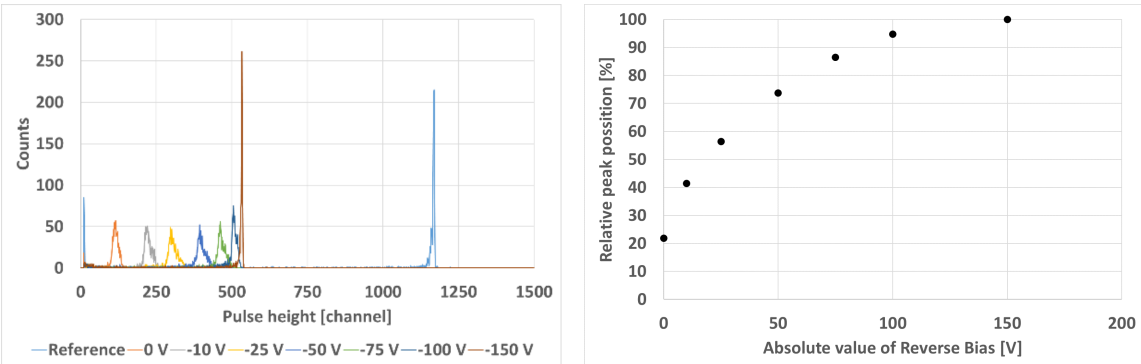

(a) **(b)**

Figure 3. (a) Dependency of a shape of a pulse height spectrum of ^{241}Am source on applied reverse bias measured with SiC strip sensor and one spectrum measured with reference Si diode for comparison. (b) The relative peak position dependency relative to the reverse bias measured with the SiC sensor.

As can be seen on figure 3(a) the resolution of the SiC diode detector is almost identical to the resolution of the Si PIN diode. The only difference is that the Si PIN diode can resolve the fine structure of ^{241}Am spectrum and the SiC cannot. The ^{241}Am spectrum consists of three peaks at 5,4827 MeV (86% relative intensity), 5,4429 MeV (12,7 %) and 5,389 MeV (1,3 %).

Performed bias scan (figure 3(b)) manifests dependency of the resolution and the charge collection efficiency of the SiC detector. It is shown that the SiC sensor is fully depleted at -150 V when the pulse height stops increasing and the resolution is the best and comparable to the Si detector. This result also indicates that the sensor is fully depleted before it reaches the breakdown and can be used within this limits.

2020 JINST 15 C01036

The sensor was also tested with a variety of gamma sources (^{60}Co, ^{137}Cs and ^{241}Am) but since the thickness of the sensitive epitaxial layer is only 50 μm the SiC is almost insensitive to these sources. This fact is crucial for the neutron detection since a neutron field produces a lot of background gamma photons and the SiC is not affected by this background. This is disadvantage of the silicon which is sensitive to gamma photons over the energies of ^{241}Am [3].

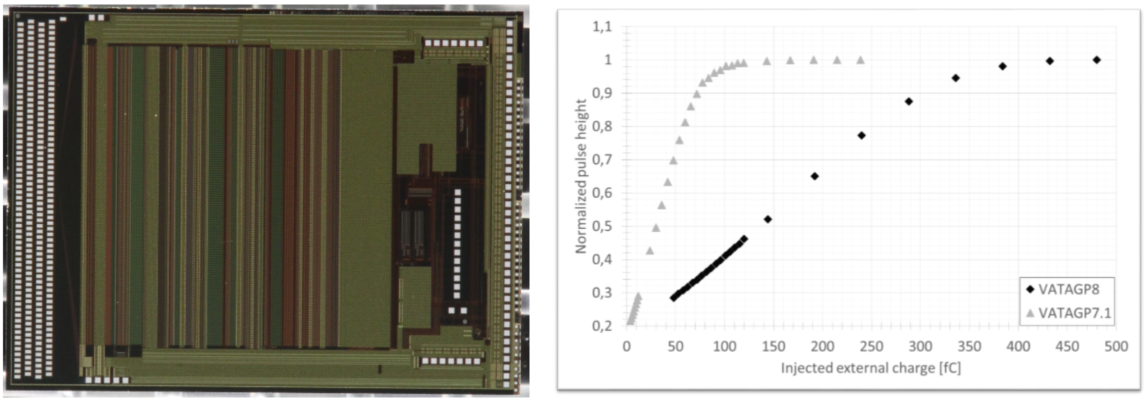

(a) **(b)**

Figure 4. (a) Photography of the VATAGP8 ASIC. (b) Output linearity versus injected charge.

4 VATA GP8 strip sensor readout

4.1 Description of the readout

The VATAGP8 is an integrated circuit (ASIC) devoted to the measurement with semiconducting sensors (figure 4(a)). The ASIC has 128 channels with low-noise and low-power buffered pre-amplifiers, shapers with sample-and-hold, and multiplexed analogue output. Each channel has a level-comparator that generates a trigger signal when the pulse-height exceeds the programmable threshold. Depending on the mode of the operation, the chip sends out the pulse height value and the address of the triggering channels, from all channels or from selected channels with the possibility to define an amount of surrounding strips to be readout. The circuit is designed to be used in parallel for reading out a large number of channels with the maximum of 16 chips on one bus with the total number of 2048 channels. The VATAGP8 has a linear charge input range up to 250 fC and can operate with positive and negative charge polarity [4].

Figure 4(b) shows results of the measurement of the input charge range of the VATAGP8 in comparison with its predecessor the VATAGP7.1. The input charge range of the VATAGP8 was extended comparing to the VATAGP7.1 to better suit the measurement of energetic charged particles mainly from neutron conversion products.

The VATAGP8 circuit was integrated into a readout board developed at IEAP CTU in Prague and assembled with the SiC sensor to form a spectrometer (figure 5(a)). Half of the sensor front side was covered with ^{6}LiF neutron converter to achieve the thermal neutron detection capability. There were two different thicknesses of the neutron converter.

2020 JINST 15 C01036

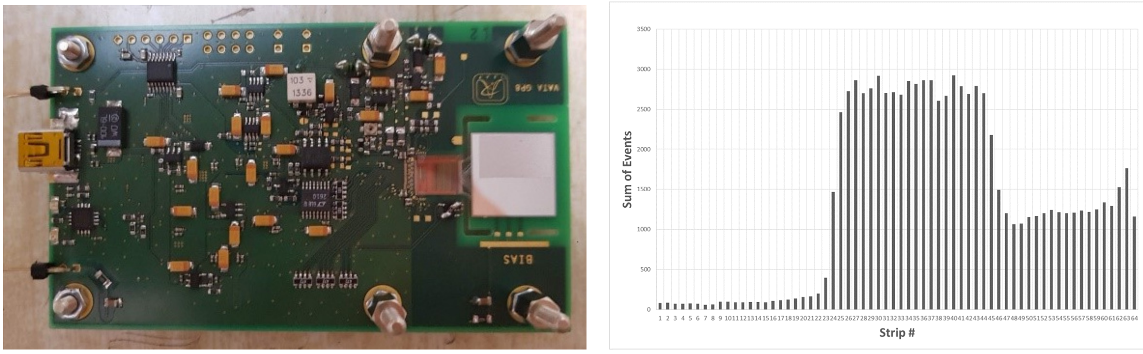

(a) **(b)**

Figure 5. (a) Photography of the assembled spectrometer with the SiC sensor and the neutron converter on top. (b) Sum of events produced by thermal neutrons and measured by the spectrometer.

4.2 Test results

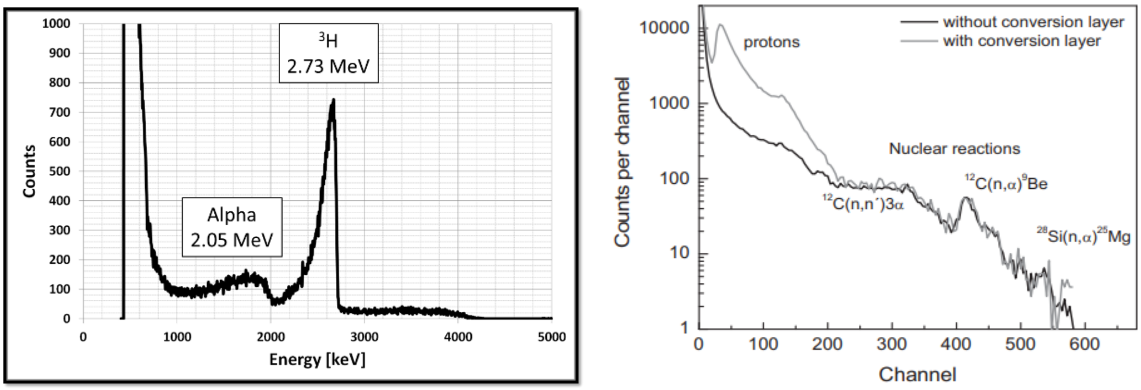

(a) **(b)**

Figure 6. (a) Events in one channel of the spectrometer with ^{6}LiF converter. (b) Fast neutron conversion spectrum with PE converter [5].

The spectrometer with the neutron converter was irradiated by thermal neutrons produced by a AmBe neutron source placed inside a PE moderator. Sum of the events recorded in each channel were plot in one graph (figure 5(b)) and clearly show the difference of thicknesses of the neutron converter.

Figure 6(a) shows spectrum of events produced by neutron conversion in the thin neutron converter which were recorded by the spectrometer. Since we used the thin film we can clearly identify events produced by neutron conversion products, alpha and triton. Figure 6(b) present a fast neutron spectra measured by B. Zatko et al. [5] in which he demonstrate a fast neutron detection capability of SiC but unfortunately we weren't able to reproduce the measurement with our spectrometer until publication of this article.

2020 JINST 15 C01036

5 Conclusions

In this article we presented an idea of the strip sensor spectrometer with capability of measurement of the heavy charged particles (alphas), thermal and fast neutrons. It was described how the strip sensor can be produced and how it should be tested. The sensor performed as expected and produced results comparable to other semiconductor sensors. Advantages of the SiC over other semiconducting materials were described. We suggested use of the VATA GP8 ASIC as integrated circuit suitable for this type of spectrometer.

Acknowledgments

The research leading to these results has received funding from the Ministry of Education, Youth and Sports within subprogram Eurostars-2 under Project Contract no. MSMT-8179/2017-1.

References

[1] RD50 collaboration, *Development of radiation hard sensors for very high luminosity colliders: CERN-RD*50 *project*, *Nucl. Instrum. Meth.* **A 511** (2003) 97.

[2] D. McGregor, M. Hammig, Y.-H. Yang, H. Gersch and R. Klann, *Design considerations for thin film coated semiconductor thermal neutron detectors — I: basics regarding alpha particle emitting neutron reactive films*, *Nucl. Instrum. Meth.* **A 500** (2003) 272.

[3] J. Jakubek, *Precise energy calibration of pixel detector working in time-over-threshold mode*, *Nucl. Instrum. Meth.* **A 633** (2011) S262.

[4] *VATAGP*8 *webpage*, https://ideas.no/products/vatagp8/.

[5] B. Zatko et al., *Neutron detection using epitaxial* 4*H-SiC detector structures*, in 2018 12th *International Conference on Advanced Semiconductor Devices and Microsystems (ASDAM)*, IEEE, October 2018.

2020 JINST 15 C01036